actuators

MDPI

Article

Analysis of Collision Types in Collaborative Robots Using Mechanism Actuated by Pneumatic Artificial Muscle

Dávid Kóczi * and József Sárosi

Department of Mechatronics and Automation, Faculty of Engineering, University of Szeged, 6720 Szeged, Hungary; sarosi@mk.u-szeged.hu
* Correspondence: koczid@mk.u-szeged.hu

Abstract: In the safety technology of collaborative robots, standards differentiate between various collision types, the identification and differentiation of which are essential for ensuring safe operation. The objective of this paper is to develop and test a mechanism actuated by artificial muscle to examine the detection of these profiles in different collision scenarios. The ISO 15066 standard distinguishes between two types of collisions: quasi-static and transient. Using a simplified model, experiments were conducted to evaluate whether sensors could identify collision types accurately. The results demonstrate the feasibility of identifying collision types through sensor data. The findings have the potential to enhance the safety of collaborative robots.

Keywords: collaborative robot; safety technology; artificial muscle; collision types; sensing technology

1. Introduction

This work addresses the question of whether a mechanical collision image can be obtained for a pneumatic artificial muscle (PAM) mechanism using different sensors. As shown in Figure 1, the ISO 15066 standard distinguishes between two types of impact. One is quasi-static collision and other is the transient collision [1].

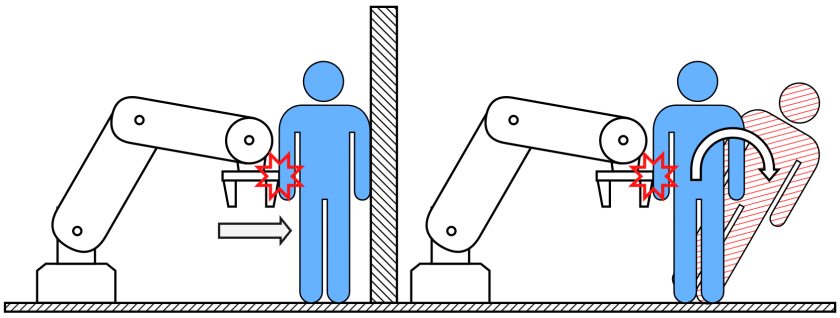

Figure 1. Quasi-static and transient contact.

For the safety of collaborative robots, it is particularly important to investigate different collision types due to the potential interaction with humans [2].

The ISO 15066 standard defines two types of possible contact:

- Quasi-static contact: "This includes clamping or crushing situations in which a person's body part is trapped between a moving part of the robot system and another

Academic Editors: Mahato Manmatha and Jaehwan Kim

Received: 17 December 2024
Revised: 6 January 2025
Accepted: 8 January 2025
Published: 10 January 2025

Citation: Kóczi, D.; Sárosi, J. Analysis of Collision Types in Collaborative Robots Using Mechanism Actuated by Pneumatic Artificial Muscle. *Actuators* **2025**, *14*, 22. https://doi.org/10.3390/act14010022

fixed or moving part of the work cell. In such a situation, the robot system would apply a pressure or force to the trapped body part for an extended time interval until the condition can be alleviated [1]."

- Transient contact: "This is also referred to as "dynamic impact" and describes a situation in which a person's body part is impacted by a moving part of the robot system and can recoil or retract from the robot without clamping or trapping the contacted body area, thus making for a short duration of the actual contact. Transient contact is dependent on the combination of the inertia of the robot, the inertia of the person's body part, and the relative speed of the two [1]".

Collaborative robots that support force- and power-limiting operations provide means to configure limiting thresholds such as forces, torques, velocities, momentum, mechanical power, axis ranges, and space ranges. To reduce the risks associated with transient contact, the speed of moving parts should be limited, and the physical characteristics of moving parts that could come into contact with the operator should be appropriately designed. To reduce the risk of quasi-static contact, speed limits and physical characteristics are similarly important, supplemented by design measures to prevent entrapment of the operator or body parts [1].

If a robot's motion has a risk of clamping or pinning a body part between the robot and another object in the cell, the robot's speed must be limited to comply with protective thresholds for the affected body area, as illustrated in Figure 2 [1].

As shown in Figure 2, different collision types are defined in the standard for collaborative robotics [3]. These are quasi-static and transient collisions, as defined above. The two types have different limits, the "transient limit" is less strict over a short time in terms of force or pressure amplitude and the "quasi-static limit" is more strict over a long time in terms of force or pressure amplitude. The fundamental difference between the two collision types is the time course of the force signals. A quasi-static collision results in a slower collision while a transient collision results in a faster "punch-like" intensity and subsequent decay [2]. However, for transient collisions with higher allowable force or pressure, the force or pressure must fall back below the quasi-static limit within 0.5 seconds of time as defined by the standard in [1].

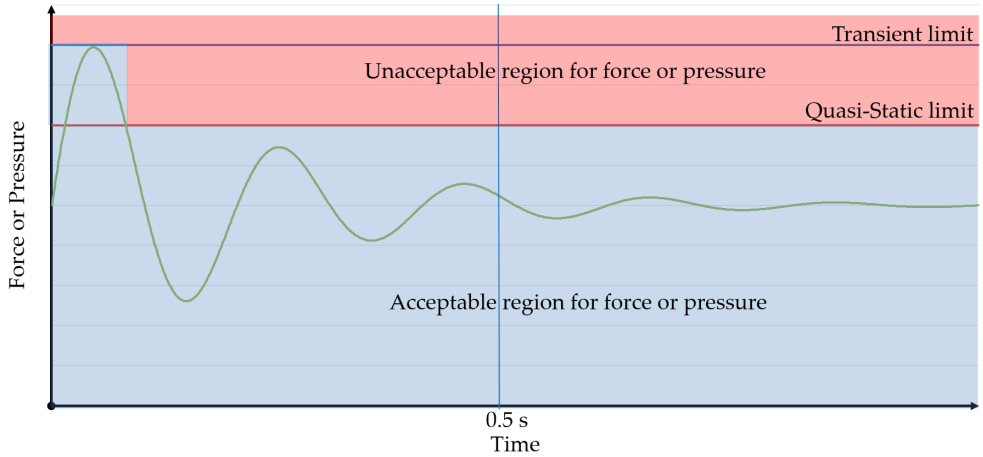

Figure 2. Graphical representation of acceptable and unacceptable forces or pressures.

These collaborative robots can be driven by different mechanisms [4]. The traditional electric servo drive is the most popular [4]. We can see a solution for a robot with a rotating work cylinder in [5]. There is a more limited but growing segment of the market for soft-actor mechanisms [6]. There are also many examples of mechanisms using PAMs [7].

A PAM, Figure 3, is a soft actuator that operates with compressed down-air similar to a reciprocating cylinder, but artificial muscles differ from reciprocating cylinders in that they have no internal moving parts and are typically lighter and simpler in construction [8].

Figure 3. Pneumatic artificial muscle (PAM).

There has been research in a number of areas to see how different types of detection help to determine the fact of a collision [9]. The most common sensing method is to test for changes in position and motor current [10]. Based on the current draw of the robot's motors, the robot can detect when it hits an obstacle because the current draw changes sharply in the event of a collision. In addition, we can also see solutions for detection with vision systems where one or more cameras can determine the spatial position of the worker and the robot and even the fact of a collision [11]. Furthermore, there is a solution called the so-called "smart skin", where the proximity of a person is detected by an inductive and capacitive sensor. The electric field reflects the physical distance of the object; the sensing area could be 0–24 mm around the skin [12]. Vibration detection is also an effective way to detect collisions. Vibration analysis enables robots to detect collisions in their environment, thus improving the safety of human–robot interaction [13].

However, one of the most effective ways to determine the impact profile is to implement force measurement [14].

A possible alternative to force measurement could be the so-called force-sensitive resistor, which allows the analysis of the given force conditions at the point of measurement [15]. These sensors also have the advantage that they can be applied not only on horizontal surfaces but also on curved or irregular surfaces due to their flexibility [16]. It is argued that the use of sensor fusion solutions to determine different collision images can improve the safety engineering of collaborative robots.

With respect to the above, the aim of this paper is to perform measurements on a simplified model where it is possible to determine the collision image with different types of sensors, which can later be used as a basis for the design of more complex devices, such as safety reactions for soft actuator-driven robots.

2. Materials and Methods

The main goal was to build the simplest possible pneumatic artificial mechanism model where one can model each collision scenario and evaluate it with the appropriate sensor data. When constructing and planning the system, efforts were made to keep it low-cost, and the availability of parts was also taken into account.

The simplified model was designed with the main objective of demonstrating, on the simplest mechanics operated with PAM, what methods might be suitable for determining the collision image. Further considerations in the design of the system were to be cost-effective and simple to implement. The system consists of a pneumatic circuit and sensors connected to it, and their electrical control circuit.

2.1. Physical Implementation

The overall pneumatic system is simple in design, as illustrated in Figure 4, starting with an air preparation unit set at a constant pressure of 0.6 MPa.

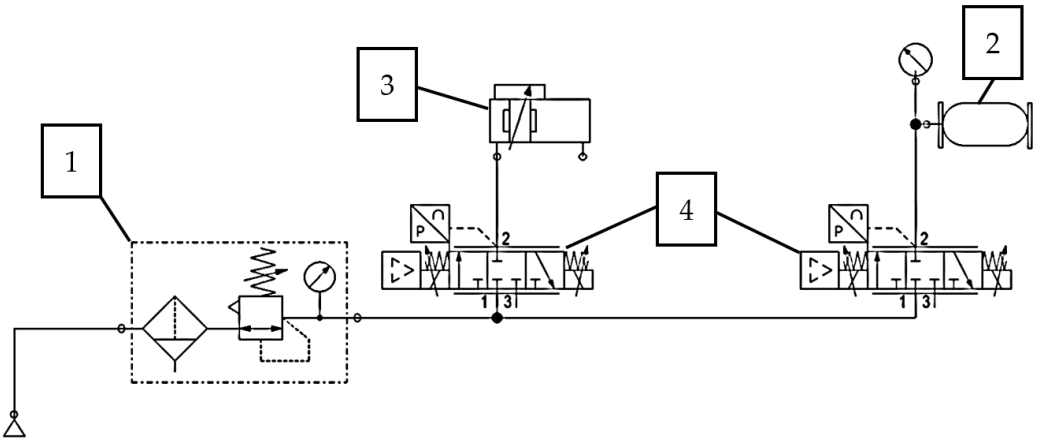

Figure 4. Pneumatic diagram: 1. air preparation unit; 2. artificial muscle: Festo MAS-10-40N-AA; 3. cylinder: Hafner PLF32; 4. proportional valve: AVENTIC Series ED02.

The target object of the measurements is the PAM, which is a 250 mm-long PAM of the type "Festo MAS-10-40N-AA". It is capable of 25% total contraction at a pressure of 0.8 MPa. The PAM is mounted on a 32 mm diameter working cylinder with a piston rod, type "Hafner PLF32", which is able to provide the necessary back-pressure force and to simulate the standing load for the measurements. These two pneumatic units are controlled by 1-1 proportional valve "AVENTICS™ Series ED02".

The measurements performed have two main focuses: One is whether each sensor can be used to determine whether a collision is quasi-static or transient. The other is which sensor can be used to determine the image of the collision. The precision force cell "S9M/1 kN" is mounted in front of the PAM by means of a ball joint. The next sensor is a "Rexroth SM6-AL" analogue distance measuring sensor mounted on a cylinder, which helps to determine the degree of contraction of the artificial muscle through the position of the cylinder piston. The third sensor is a "Festo SPTE-571484" analogue pressure transducer. The force sensitive resistor "Legact FSR RP-C18,3-LT" is used to directly detect the impact.

Figure 5 shows the experimental setup designed for analysing collision types. The figure illustrates the integration of a PAM and its connection to the supporting components, enabling the simulation of both quasi-static and transient collisions. The setup includes a linear motion mechanism for controlled impact generation and precise measurement of collision forces. This configuration allows for detailed evaluation of sensor performance in detecting and distinguishing collision types, ensuring accurate data collection and analysis. The measurement is performed with the point of collision marked in red. The object impacted by the mechanism can be fixed or positioned to allow movement, simulating whether the collision type is quasi-static or transient.

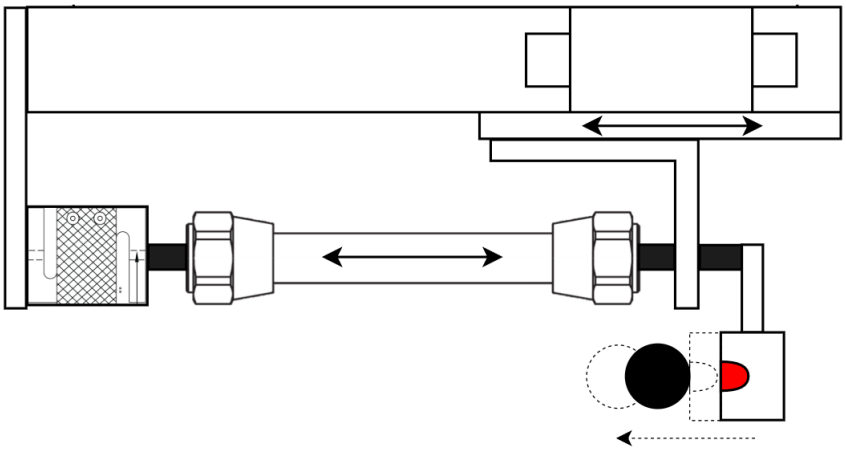

Figure 5. Experimental setup for collision type analysis using PAM.

Figure 6 shows pictures of the completed measurement system. To test the sensors and to perform a large number of measurements, a clampable steel cylinder was selected, weighing 600 g and designed to be rigidly clamped and freely movable as required, as shown in Figure 6a,b.

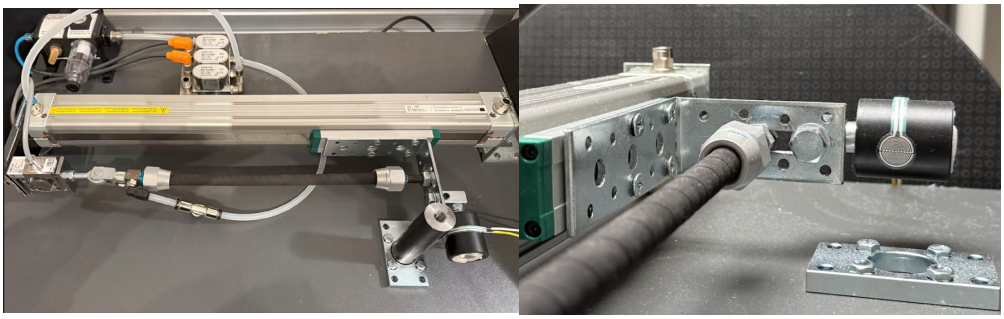

(**a**) (**b**)

Figure 6. Measurement system: (**a**) picture of assembled measurement system; (**b**) collision surface with sensor.

2.2. Control System

The control core is an NI myRIO-1900 controller. This unit has a triple role. This unit is responsible for processing/converting the incoming signals and controls the proportional valves via the outputs, and also stores and sends the data to the PC. The system voltage interfaces are implemented with a laboratory power supply and simple circuit elements. Figure 7 illustrates the inputs and outputs of the system.

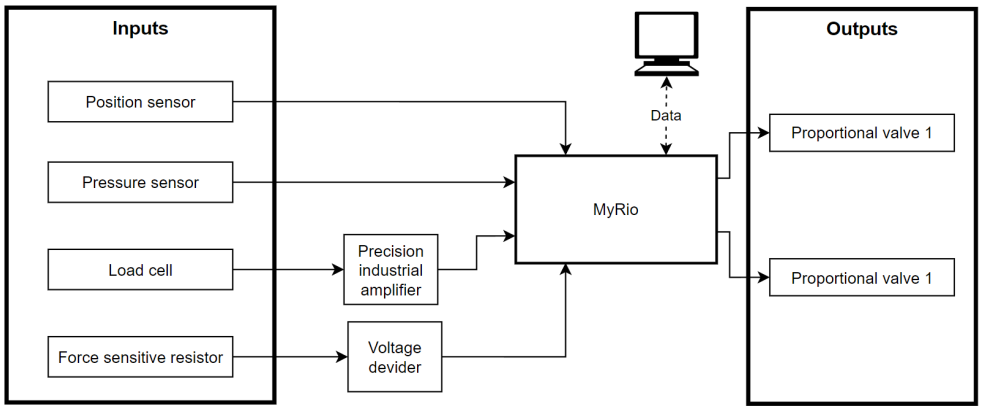

Figure 7. Input/output diagram.

The control software was developed in the LabVIEW (NI Labview 2019) programming environment and its structure is illustrated in Figure 8. The control is designed to save a preset data length when the moment of impact is detected. The necessary control and display elements are divided into four main parts in the figure. The first part of the control interface contains the sensor data, a stopping sphere, and a bar representing the position of the working cylinder. In the second part, the slider in yellow allows the preload to be set in MPa and the preload value to be returned in N. The blue bar is used to adjust the PAM pressure in MPA. As previously indicated the maximum pressure of the system is set to 0,6 MPa, so the tests were performed at this pressure value. In the section marked with 3, the graphical representation can be seen through diagrams and various visualisation elements. In the section marked with 4, we find the trigger point setting variable; as mentioned earlier, this is the stress value that, when measured on the force-resistive sensor, indicates the start of the measurement, i.e., the moment of impact. The other variable is used to set the sampling rate, which at the current setting corresponds to a sampling rate of 10 ms.

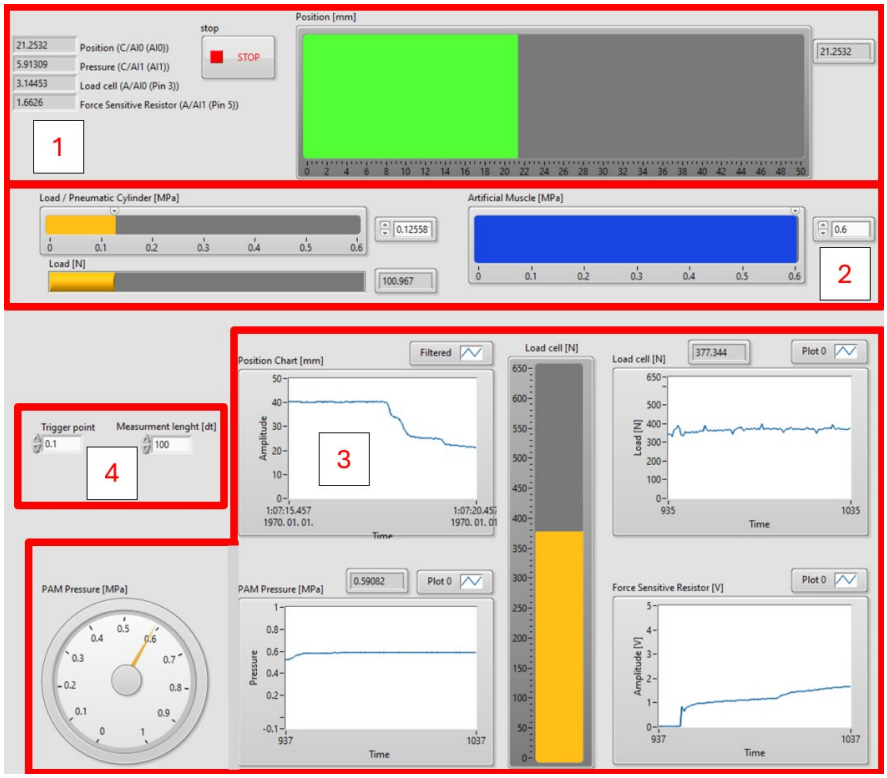

Figure 8. LabVIEW user interface.

2.3. Theoretical Background

The PAM-based mechanism provided a simple and efficient tool for simulating and testing different collision scenarios. During the test, fir key parameters of the system, such as the sensed force on the cell and the force-sensitive resistor, both pressure and distance were measured and evaluated using mathematical methods.

The force–time characteristics of a quasi-static collision can be described by the following mathematical formula:

$$F_s(t) = \begin{cases} F_{\max} \cdot \dfrac{t}{t_{\max}} \text{ if } 0 \le t \le t_{\max} \\ F_{\max} \cdot \left(1 - \dfrac{t - t_{\max}}{t_{\mathrm{d}}}\right) if\ t_{\max} < t \le t_{\max} + t_d \end{cases} \quad (1)$$

where F_s: quasi-static collision force; $F_{\max}$: collision force maximum; $t_{\max}$: time to peak of force; and t_d: the damping period.

During a transient collision, the force is characterised by an exponential decrease:

$$F_t(t) = F_{\max} \cdot e^{-\frac{t}{\tau}} \quad (2)$$

where F_t: transient collision force; τ: the time constant of the collision, which characterises the speed.

The force output of a PAM is described by the following formula [17]:

$$F_{PAM} = P \cdot A \cdot (a \cdot (1 - \varepsilon \cdot k)^2 - b) \quad (3)$$

where F_{PAM}: force generated by the muscle; P: internal pressure (Pa); A: useful cross-measures of the muscle; ε: effective surface area; k: contraction; a and b: estimated PAM-specific constants.

Furthermore, an important context for the analysis of the data obtained is the calculation of the simplified Pearson coefficient [18]:

$$r = \frac{n(\sum xy) - (\sum x) \cdot (\sum y)}{\sqrt{(n\sum x^2 - (\sum x)^2) \cdot (n\sum y^2 - (\sum y)^2)}} \quad (4)$$

where x and y: variables to be compared; n: number of data points.

2.4. Measurement Method

In order to carry out the measurements, the scenarios shown in Table 1 below were defined.

Table 1. Measurement scenarios with preload.

No.	Static Collision	Transient Collision
1	0 N	0 N
2	10 N	10 N
3	50 N	50 N
4	150 N	150 N
5	200 N	200 N

The quasi-static collision scenario means that the metal cylinder was fixed in the system and that is how the collision occurred. In contrast, in a transient collision, the system has the possibility to move/push the rod.

All measurements were taken at the moment of impact, helping a later development to relate the response to the detection. For the quasi-static collision type, 10 measurements were taken in each scenario, and for the transient collision type, 10 measurements were taken in each scenario. The measurements were taken with a sampling time of 10 ms and a duration of 1 s. The values of each of the four sensors were stored separately to facilitate analysis.

3. Results

All measurement results for each scenario are summarised in a table. The average of these measurements is summarised in the following charts.

The position sensor data are shown in Figure 9. By comparing the transient and static cases, we can see that the difference between the two collision types is clearly visible. In the static case, the position varies in a small range due to the preload stretching the PAM and thus the magnitude of the distance travelled varies proportionally. In the transient case, the system can travel almost the entire distance.

One value I would like to highlight, in both cases, is the value measured at 200 N preload. In this case, the PAM can hardly move/accelerate from this stretched state. This will also be true for the measurements of the other sensors.

Overall, however, it can be seen from the results that when approaching a limit stop, it is not possible to stall only due to position based on the type of collision, as the values are steady in the transient case.

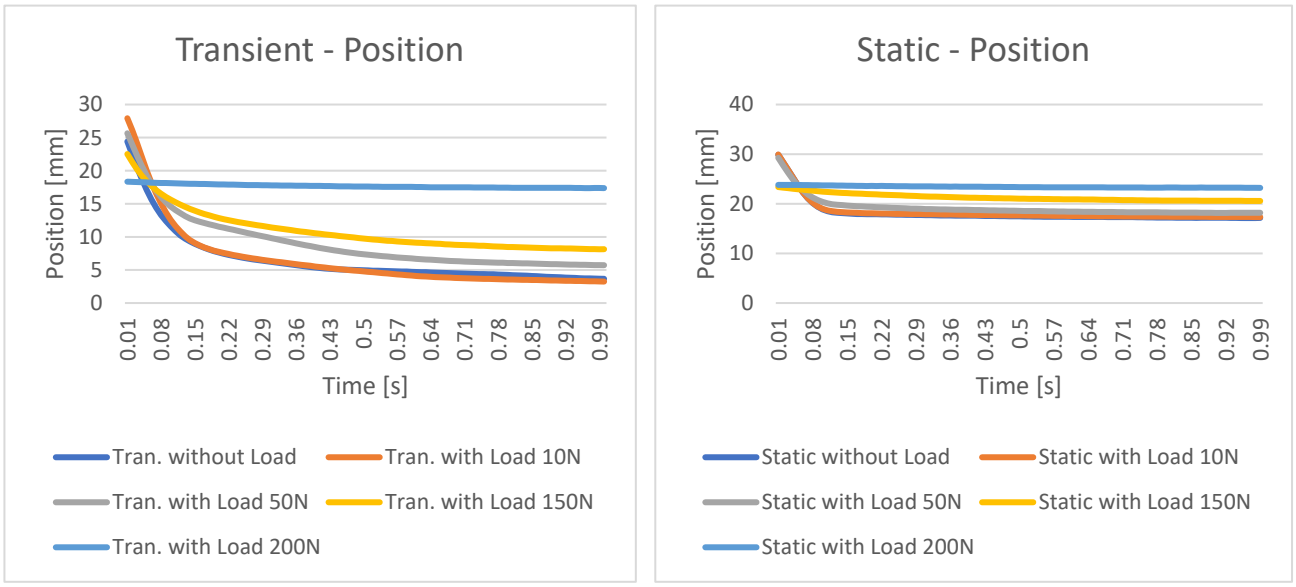

(**a**) (**b**)

Figure 9. Position measurement results. (**a**) PAM contraction/time diagram for transient collision; (**b**) PAM contraction/time diagram for static collision.

Figure 10 illustrates the pressure change in the artificial muscle over the duration of the collision. It is easy to see that there is no significant difference in the pressure value in the artificial muscle between the collision cases. By examining the pressure at this pressure and over this range, all that is obtained is that the system has reached the set value of 0.6 MPa in all cases.

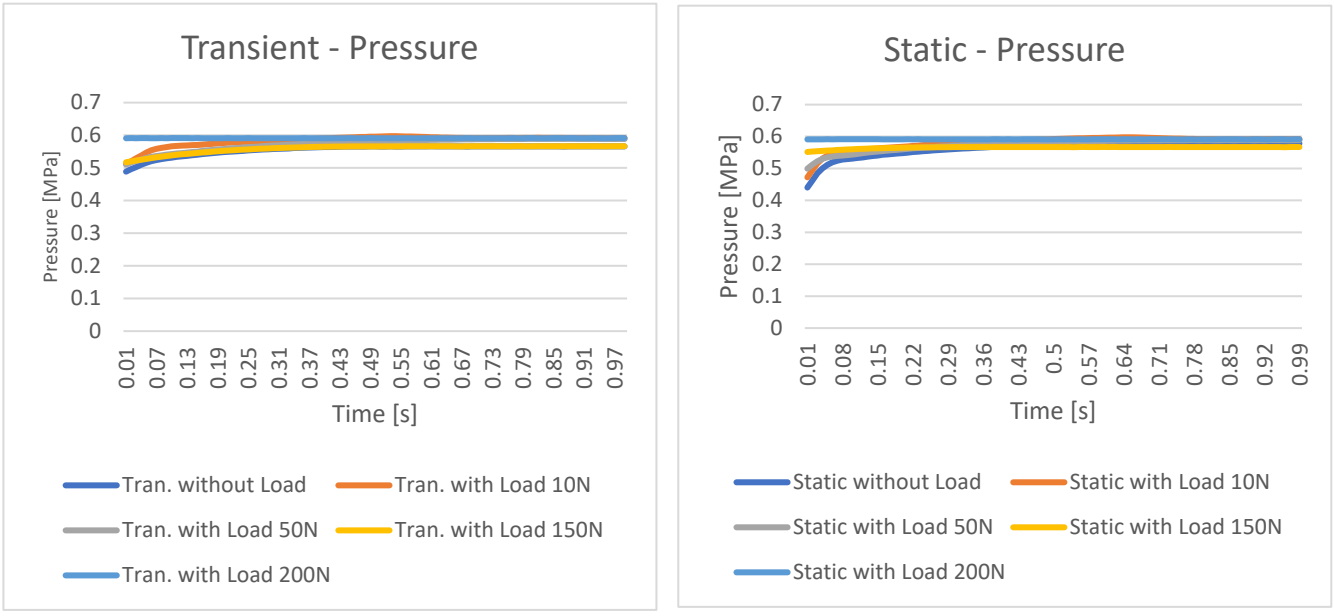

(**a**) (**b**)

Figure 10. Pressure measurement results. (**a**) PAM pressure change/time diagram for transient collision; (**b**) PAM pressure change/time diagram for static collision.

Figure 11 illustrates the variation in the force cell values over time. Here, the two types of collision are clearly visible. Since the measurement starts at the moment of collision, we can see that in the transient case, the steady state is already measured on the cell and the preloads are nicely plotted. In the static case, the increasing force lines are nicely drawn.

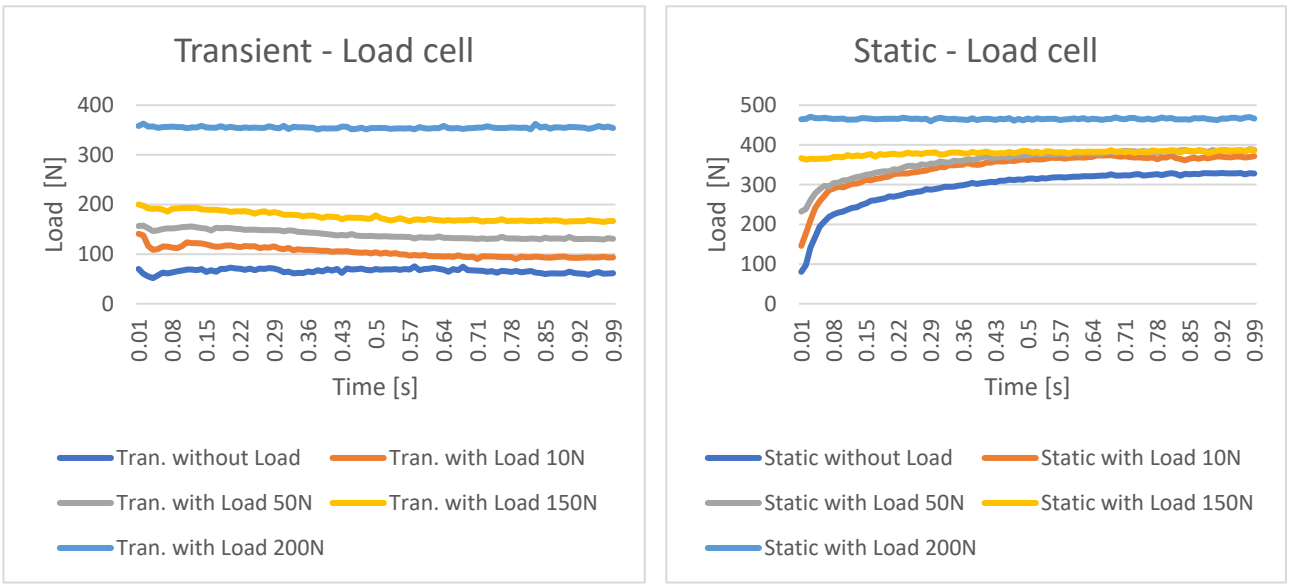

(**a**) (**b**)

Figure 11. Measurement results of a load cell. (**a**) PAM force–time diagram for transient collision; (**b**) PAM force–time diagram for static collision.

Figure 12 illustrates the change in the sensitive sensor's time response to force at the collision boundary. Observing the results, what can be pointed out at first glance is that due to the lower forces, the voltage values read from the diagram are lower for transient collisions between 0 and 1.2 V, and even in the static case the result goes towards 3 V. The next thing that is clearly visible is that at a load of 150 N the signal loses its linearity, which is due to the fact that the preload causes the contraction to lose speed, so the cylinder may not be pushed off immediately, but just thrown off balance, and in turn slams back onto the sensor surface. At a load of 200 N, the signal does not lose its linearity because the PAM reaches a near-maximum contraction state. This limits further movement, thereby reducing dynamic effects such as overshoot or rebound. As a result, the system operates closer to a quasi-static state, where the preload force dominates.

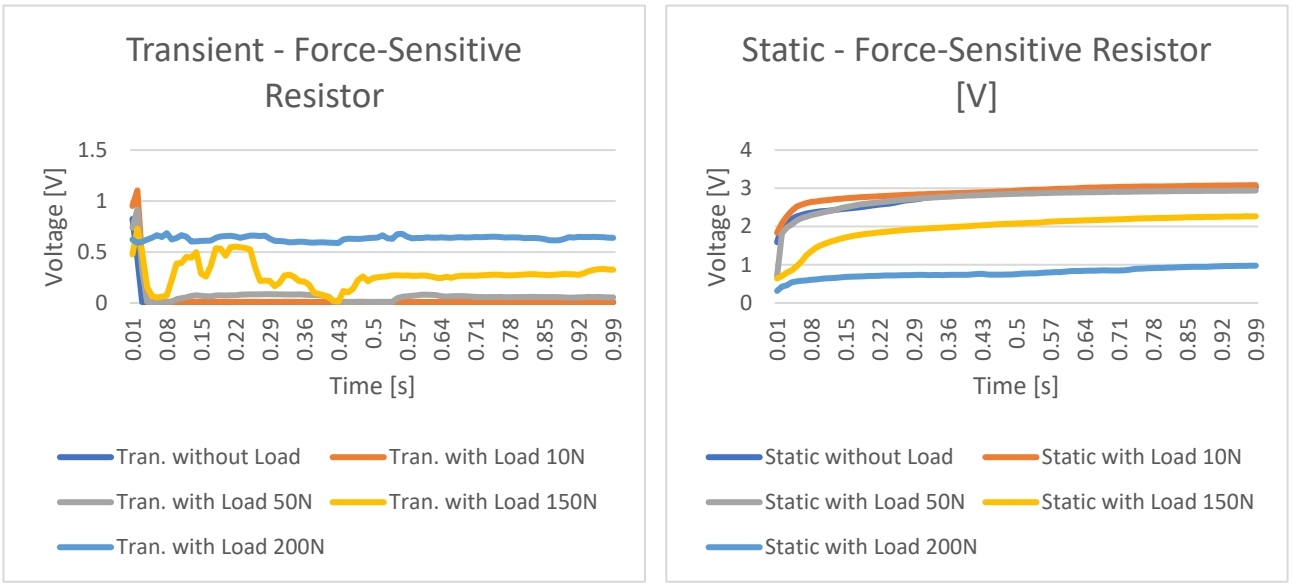

(**a**) (**b**)

Figure 12. Force-sensitive resistor measurement results. (**a**) PAM voltage–time diagram for transient collision; (**b**) PAM voltage–time diagram for static collision.

A correlation study between the load cell and force-sensitive values is worthwhile, as the latter can be a much more cost-effective solution than a precision force-measuring cell. The correlation between the values of the two sensors is shown in Table 2.

Table 2. Pearson correlation values between load cell and force-sensitive resistor values.

Preload	Static Correlation	Transient Correlation
0 N	0.974038	0.107883
10 N	0.971619	0.460071
50 N	0.948798	0.263943
150 N	0.926691	0.363808
200 N	−0.06596	−0.0293

Table 2 shows that in the case of a static collision, the values show high linearity, and there is even more correlation in the case of a transient collision. At high loads, no linear correlation between the values can be interpreted.

The cost-effectiveness of the system was primarily achieved using a force-sensitive resistor instead of traditional precision force-measuring cells. Force-sensitive resistors are significantly less expensive, with costs up to an order of magnitude lower, while still providing sufficient accuracy for the intended collision type differentiation.

4. Discussion

The results show that the differential analysis of quasi-static and transient collisions can be accurately performed in a PAM-based system. This approach is particularly relevant for safety engineering of collaborative robots.

The experiments successfully demonstrated the capability of PAM-based systems to distinguish between quasi-static and transient collisions. The findings validate the potential of PAM mechanisms with a force-sensitive resistor as cost-effective and efficient alternatives for collision detection and safety enhancement in collaborative robotics.

Furthermore, the use of a simplified model allowed for a clear demonstration of the feasibility of various sensors in identifying collision types.

Among these, the force-sensitive resistor sensor showed promise as a cost-efficient alternative to precision force-measuring cells. Force sensitive resistors are significantly less expensive, with costs up to an order of magnitude lower, while still providing sufficient accuracy for the intended collision type differentiation.

The results also highlight the importance of understanding the impact of preload conditions on collision profiles. At higher preloads, the limited movement of the PAM affected the accuracy of the collision type classification. This emphasizes the need for further investigations under dynamic and real-world conditions, such as varying impact surfaces and additional sensor variations, to enhance the robustness of the proposed system. At high preloads, the PAM's ability to move was limited, which affected the accuracy of the impact profiles.

The correlation analysis between force sensors and force-sensitive resistor sensors has highlighted that more cost-effective force-sensitive resistor sensors may be a suitable alternative to precision force-sensing cells in some cases.

The current studies were performed under fixed conditions; further analysis of more dynamic or real application situations is needed, such as impact surface and testing of additional sensor variations.

A safety response based on these indications can then be developed.

5. Conclusions

- Tests have shown that PAM-based systems are not only able to detect collisions but are also able to distinguish between collision types. This is essential for the safe operation of collaborative robots.
- Force-sensitive resistor sensors offer a cost-effective alternative to force measurement cells, subject to certain limitations. However, a deeper understanding of the effects of preload is essential.
- The results suggest the use of sensor solutions for the integration of PAM systems in collaborative robotics applications, especially in environments where fast reactions and human–robot interactions are of high importance.

Author Contributions: Conceptualization, D.K. and J.S.; writing—review and editing, D.K. and J.S. All authors have read and agreed to the published version of the manuscript.

Funding: This research received no external funding.

Data Availability Statement: Data are contained within the article.

Conflicts of Interest: The authors declare no conflicts of interest.

References

1. ISO TS 15066_EN. Available online: https://www.iso.org/standard/62996.html (accessed on 16 December 2024).
2. Samarathunga, S.M.B.P.B.; Valori, M.; Faglia, R.; Fassi, I.; Legnani, G. Considerations on the Dynamics of Biofidelic Sensors in the Assessment of Human–Robot Impacts. *Machines* **2023**, *12*, 26. https://doi.org/10.3390/machines12010026.
3. Kang, Y.; Kim, D.; Yun, D. Manipulator Collision Avoidance System Based on a 3D Potential Field With ISO 15066. *IEEE Access* **2022**, *10*, 126593–126602. https://doi.org/10.1109/ACCESS.2022.3221182.
4. Requirements for Safe Robots: Measurements, Analysis and New Insights. Available online: https://journals.sagepub.com/doi/epdf/10.1177/0278364909343970 (accessed on 15 December 2024).
5. Olszewski, M. Modern Industrial Robotics. *Pomiary Autom. Robot.* **2020**, *24*, 5–20. https://doi.org/10.14313/PAR_235/5.
6. El-Atab, N.; Mishra, R.B.; Al-Modaf, F.; Joharji, L.; Alsharif, A.A.; Alamoudi, H.; Diaz, M.; Qaiser, N.; Hussain, M.M. Soft Actuators for Soft Robotic Applications: A Review. *Adv. Intell. Syst.* **2020**, *2*, 2000128. https://doi.org/10.1002/aisy.202000128.
7. A Seven-Degrees-of-Freedom Robot-Arm Driven by Pneumatic Artificial Muscles for Humanoid Robots. Available online: https://journals.sagepub.com/doi/epdf/10.1177/0278364905052437 (accessed on 15 December 2024).

8. Sarosi, J.; Biro, I.; Nemeth, J.; Cveticanin, L. Dynamic modeling of a pneumatic muscle actuator with two-direction motion. *Mech. Mach. Theory* **2015**, *85*, 25–34. https://doi.org/10.1016/j.mechmachtheory.2014.11.006.
9. Safeea, M.; Neto, P.; Bearee, R. On-line collision avoidance for collaborative robot manipulators by adjusting off-line generated paths: An industrial use case. *Robot. Auton. Syst.* **2019**, *119*, 278–288. https://doi.org/10.1016/j.robot.2019.07.013.
10. Ollero, A.; Sanfeliu, A.; Montano, L.; Lau, N.; Cardeira, C. (Eds.) *ROBOT 2017: Third Iberian Robotics Conference: Volume 2*; Advances in Intelligent Systems and Computing; Springer International Publishing: Cham, Switzerland, 2018; Volume 694. https://doi.org/10.1007/978-3-319-70836-2.
11. Schmidt, B.; Wang, L. Depth camera based collision avoidance via active robot control. *J. Manuf. Syst.* **2014**, *33*, 711–718. https://doi.org/10.1016/j.jmsy.2014.04.004.
12. Pang, G.; Yang, G.; Pang, Z. Review of Robot Skin: A Potential Enabler for Safe Collaboration, Immersive Teleoperation, and Affective Interaction of Future Collaborative Robots. *IEEE Trans. Med. Robot. Bionics* **2021**, *3*, 681–700. https://doi.org/10.1109/TMRB.2021.3097252.
13. Villani, V.; Fenech, G.; Fabbricatore, M.; Secchi, C. Wrist Vibration Feedback to Improve Operator Awareness in Collaborative Robotics. *J. Intell. Robot. Syst.* **2023**, *109*, 45. https://doi.org/10.1007/s10846-023-01974-4.
14. Yen, S.-H.; Tang, P.-C.; Lin, Y.-C.; Lin, C.-Y. Development of a Virtual Force Sensor for a Low-Cost Collaborative Robot and Applications to Safety Control. *Sensors* **2019**, *19*, 2603. https://doi.org/10.3390/s19112603.
15. Giovanelli, D.; Farella, E. Force Sensing Resistor and Evaluation of Technology for Wearable Body Pressure Sensing. *J. Sens.* **2016**, *2016*, 9391850. https://doi.org/10.1155/2016/9391850.
16. Zhu, Y.; Liu, Y.; Sun, Y.; Zhang, Y.; Ding, G. Recent Advances in Resistive Sensor Technology for Tactile Perception: A Review. *IEEE Sens. J.* **2022**, *22*, 15635–15649. https://doi.org/10.1109/JSEN.2022.3179015.
17. Sárosi, J. Pneumatikus Mesterséges Izmok Működésének Statikus és Dinamikus Modellezése, Nagypontosságú Pozicionálása. Ph.D. Thesis, Szent István Egyetem, Gödöllő, Hungary, 2013.
18. Benesty, J.; Chen, J.; Huang, Y.; Cohen, I. Pearson Correlation Coefficient. In *Noise Reduction in Speech Processing*; Springer Topics in Signal Processing; Springer: Berlin/Heidelberg, Germany, 2009; Volume 2, pp. 1–4. https://doi.org/10.1007/978-3-642-00296-0_5.